ANALYSIS OF METALLURGICAL PHENOMENA IN ISO 5832-9 STEEL SUBJECTED TO HOT TORSION

João Marcos da Silva Nunes [1] (nunesjoao@acad.ifma.edu.br), Marcelly Cristiny Nunes de Carvalho [2] (marcellyc@acad.ifma.edu.br), Isaac Araújo Furtado [2] (isaaca@acad.ifma.edu.br), Samuel Filgueiras Rodrigues [1] (samuel.filgueiras@ifma.edu.br), Eden Santos Silva [1] (eden.silva@ifma.edu.br)

[1] Instituto Federal do Maranhão (IFMA); Programa de Pós-Graduação em Ciência e Tecnologia de Materiais
[2] Instituto Federal do Maranhão (IFMA); Departamento de Mecânica e Materiais

ABSTRACT: *In the manufacturing of metal alloys, different processing methods are used to achieve desired mechanical properties. Thermomechanical processes involve phenomena such as work hardening (WH), dynamic recovery (DRV), and dynamic recrystallization (DRX), which influence the properties of the materials. However, replicating these processes on a laboratory scale is challenging due to the differences in conditions compared to the industrial scale and the high costs involved. Hot torsion machines are essential tools in simulating these processes, allowing for the study of microstructural evolution and parameter measurements. This article aims to physically simulate thermomechanical processing by hot torsion considering a strain rate of 1.0 s^{-1} and five testing temperatures. The analytical methods proposed by Poliak-Jonas and Uesugi et al. were used to determine characteristic points of the flow curves and the occurrence of metallurgical phenomena. The alloy used was austenitic stainless-steel ISO 5832-9, which is utilized for orthopedic implants. Results show that temperature has a considerable influence on the shape of the curves, as well as on the DRV and DRX phenomena, which, in turn, are influenced by the stacking fault energy.*

KEYWORDS: *THERMOMECHANICAL PROCESSING, DYNAMIC RECOVERY (DRV), DYNAMIC RECRYSTALLIZATION (DRX), STACKING FAULT ENERGY.*

ANÁLISE DOS FENÔMENOS METALÚRGICOS NO AÇO ISO 5832-9 SUBMETIDO A TORÇÃO A QUENTE

RESUMO: *Na manufatura de ligas metálicas, diferentes métodos de processamento são utilizados para alcançar propriedades mecânicas desejadas. Os processos termomecânicos envolvem fenômenos de encruamento (WH), recuperação dinâmica (DRV) e recristalização dinâmica (DRX), influenciando as propriedades dos materiais. No entanto, replicá-los em escala laboratorial é desafiador devido às diferenças nas condições em relação à escala industrial e do alto custo envolvido. As máquinas de torção a quente são ferramentas essenciais na simulação desses processos, permitindo o estudo da evolução microestrutural e medições de parâmetros. Esse artigo objetiva simular fisicamente o processamento termomecânico por torção a quente considerando uma taxa de deformação de 1,0 s^{-1} e cinco temperaturas de ensaio. Foram utilizados os métodos analíticos propostos por Poliak-Jonas e Uesugi et al. para determinação de pontos característicos das curvas de escoamento e atuação dos fenômenos metalúrgicos. A liga utilizada foi aço inoxidável austenítico ISO 5832-9 utilizada para implantes ortopédicos. Resultados mostram que a temperatura tem considerável influência no formato das curvas, assim como nos fenômenos de DRV e DRX, que, por sua vez, são influenciados pela energia de falha de empilhamento.*

PALAVRAS-CHAVE: *PROCESSAMENTO TERMOMECÂNICO, RECUPERAÇÃO DINÂMICA (DRV), RECRISTALIZAÇÃO DINÂMICA (DRX), ENERGIA DE FALHA DE EMPILHAMENTO.*

1. INTRODUCTION

During the manufacturing of metallic products, thermomechanical processes are used to shape the product and achieve the desired mechanical properties. The production of these materials requires processes that combine lower cost and high quality. Therefore, basic and technological research in materials engineering aims to understand the metallurgical phenomena that govern microstructure formation, as well as the variation in their mechanical properties, focusing on how temperature and strain rate parameters influence the final characteristics.

In thermomechanical processing, three main phenomena control the thermomechanical behavior of the metal: work hardening, dynamic recovery, and dynamic recrystallization. The mechanical-microstructural characterizations of these processes are important because they allow: (i) studying the stress-strain curves through physical simulation, developing new routes; (ii) parameterizing the active phenomena with process optimization; (iii) simulating industrial tests through physical-mathematical modeling on a laboratory scale, aiming to improve the properties (Gerônimo, 2014).

FIGURE 1. Typical thermomechanical processing routes for austenitic stainless steels.

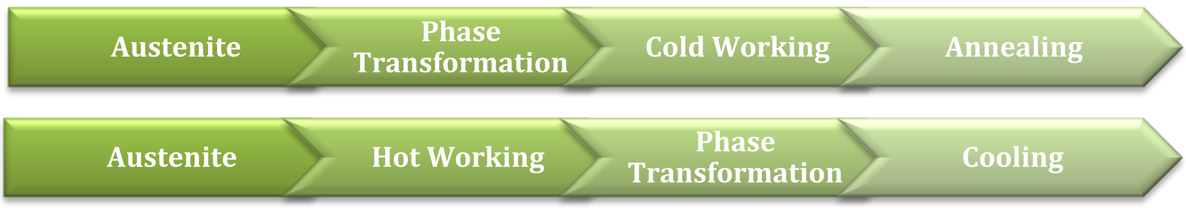

Source: Author (2024).

The processing routes directly influence the properties of metallic components, and therefore, studies are needed to discuss the fundamentals of the physical simulation of thermomechanical processing based on scientific concepts and experimental feasibility, as this processing represents a significant portion of the work done in the manufacturing of semi-finished components (Balancin, 2012). An example of a traditional thermomechanical processing route used for austenitic stainless steels is shown in Figure 1.

The hot rolling process is a metallurgical process in which metals, in the form of ingots or bars, are heated above their recrystallization temperature and successively deformed. Due to the recrystallization process, there will be a reduction in the average grain size. In hot forging, mechanical shaping is performed, which is a method for producing high-performance components with complex geometry, combining high mechanical strength and elevated toughness. In this process, the material is also heated above the recrystallization temperature, allowing for large deformations, less effort, dimensional precision, and better mechanical strength (Silva, 2011).

Although processing routes have their own characteristics, they all share common parameters. Initially, metals are heated to high temperatures, then subjected to sequences of deformations, and subsequently cooled to room temperature. It is noteworthy that the evolution of the microstructure depends on how it is initially configured, the deformation conditions, and the cooling rate, described by: temperature, sequence of passes, amount of deformation, strain rate, and time between passes or their values over time. In hot deformations, part of the energy expended is stored in the crystal lattice as defects, which are eliminated due to the work hardening-recovery or work hardening-recrystallization combination, generating a non-deformed state. Depending on the dominant phenomenon, a product with better performance and higher quality is produced (Silva *et al.*, 2012).

Analyzing the events that occur during metallurgical processes is challenging because the use of standard equipment is not economically viable due to the large size of the industrial plant. Furthermore, even on a laboratory scale, friction/lubrication conditions and heat transfer differ from those on a real scale. The inability to replicate these processes on a smaller scale led to the establishment of physical simulation, which consists of virtually reproducing the industrial process with the aid of computational constitutive models. In laboratory simulation, a reduced-sized specimen is used, on which thermomechanical cycles are imposed using equipment capable of varying the parameters on a large scale, with simultaneous recording of the material's response to the imposed parameters. Figure 2 shows the stages of physical simulation (Sulzbach *et al.*, 2022).

FIGURE 2. Stages of the physical simulation.

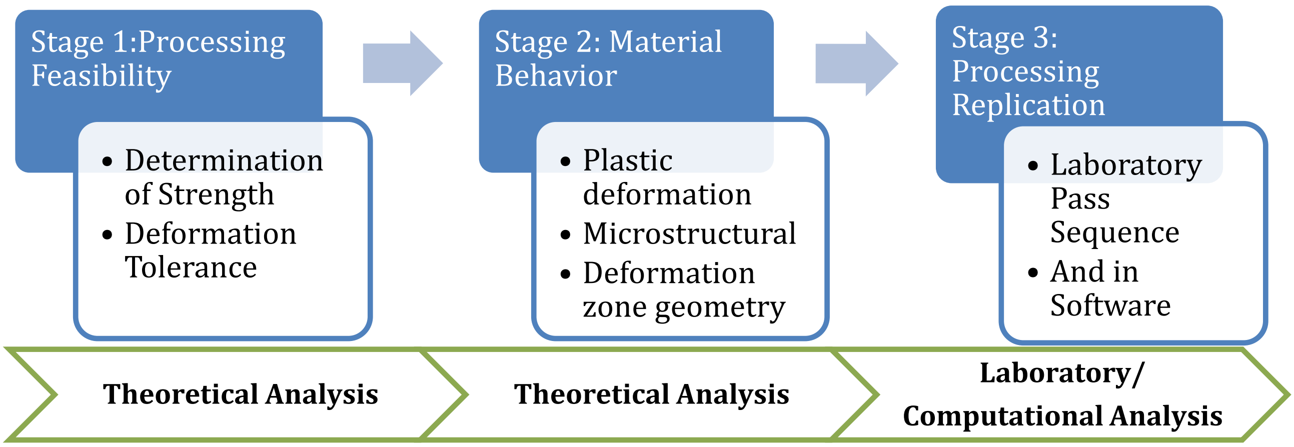

Source: Author (2024).

Among the various laboratory methods used for the physical simulation of industrial processing, the hot torsion test stands out. The specimen developed for the test is shown in Figure 3. In this test, one end of the cylindrical specimen is kept fixed, while the other is subjected to a rotational force. The events that occur during the physical simulation are investigated using stress-strain curves and monitoring the microstructural evolution. The stress-strain curves for the surface of twisted cylindrical samples are calculated from the torque and rotation angle using the relations (Fields and Backofen, 1957):

FIGURE 3. Representation of the specimen for a hot torsion test.

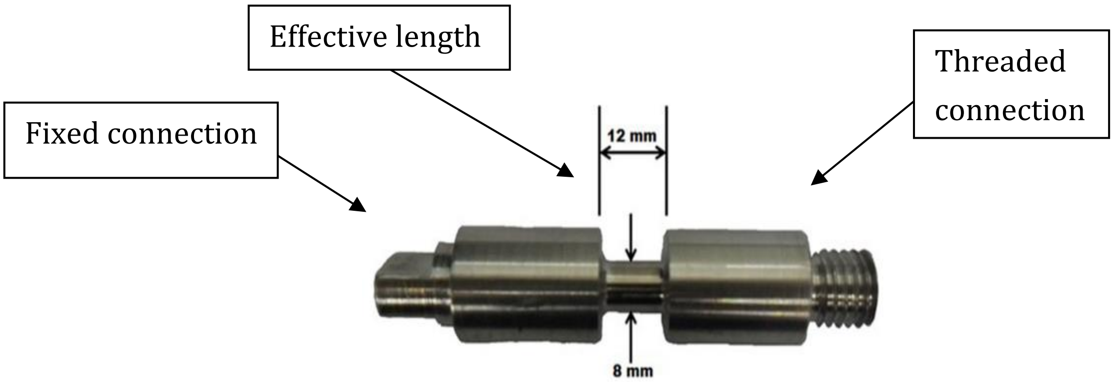

Source: Author (2024).

With multiple deformation tests, it is possible to replicate industrial processing and investigate the mechanisms that act during the time between passes. Thus, it is possible to evaluate the role of work hardening and softening mechanisms, as well as design and investigate the sequence of passes that optimize the properties of the metal implemented industrially.

Figure 4 shows the requirements for simulating an industrial process in the laboratory. It is the portion of microstructural changes due to entropy production that leads to variations in the effort applied by the machine.

FIGURE 4. Basic functions of an industrial processing in the laboratory.

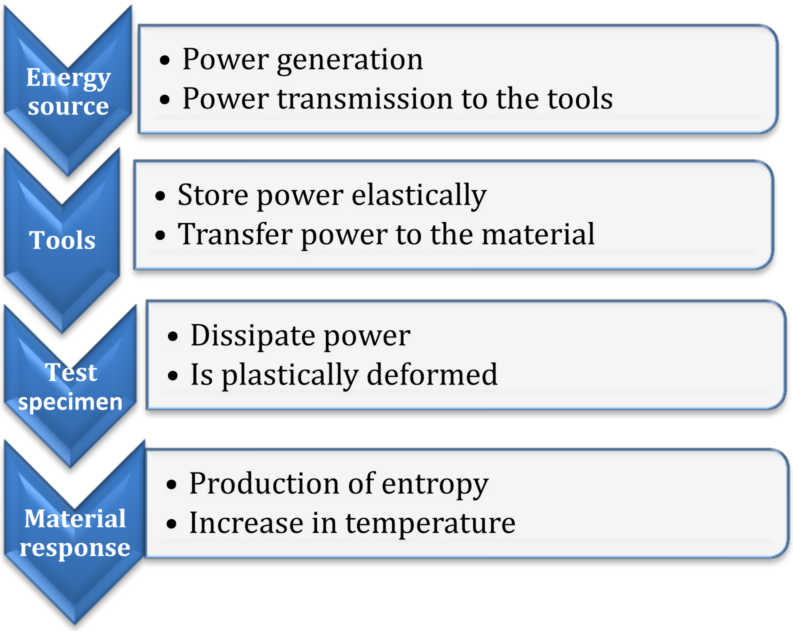

Source: Author (2024).

1.1 Operation of the Hot Torsion Machine

The hot torsion machine consists of a motor, brake, and clutch, which determine the deformation speed in each pass and the start and end of each deformation. The thermal cycle is carried out by an infrared radiation furnace attached to the machine, which must be programmed to replicate industrial thermomechanical treatments. The electric servomotor has variable speed, and the mechanical forces applied to the specimen are measured by a variable load cell and converted into equivalent stress. Temperature control in the furnace is provided by thermocouples.

The deformation and strain rate are calculated from measurements of the rotation angle by a digital optical rotation transducer. Data acquisition is performed by a computer interfaced with the machine, where software controls the tests. To prevent oxidation of the specimen and impose different cooling rates during physical simulation, inert gases or coolants can be injected through a quartz tube. Water can also be injected through the tube if quenching is desired for analyzing microstructural evolution.

FIGURE 5. Three generations of hot torsion machines.

Source: Author (2024).

Figure 5 schematically shows three generations of the computerized horizontal hot torsion machine developed by the thermomechanical processing research group in Brazil at PPGEM/UFSCar under the coordination of Professor Dr. Oscar Balancin. The hot torsion machine began as a prototype in 1984, titled "Development of a Prototype for Hot Torsion Tests - CNPq Proc. no. 40.6783/84. 1984."

1.2 Metallurgical Phenomena During Hot Deformation

1.2.1 Work Hardening (WH)

The metallurgical phenomenon of work hardening is the mechanism responsible for rising the mechanical strength of metals during the plastic deformation, and its existence depends on the variation of deformation and the applied temperature. In thermomechanical treatments, this mechanism occurs due to the elevation in the number of dislocations during the application of stress. The dislocations formed organize into cellular structures and subgrains that, with increased deformation, will convert into refined grains, contributing to the mechanical strength of the metal (Jorge, 1997).

Effective work hardening can be assessed by the initial slope of the plastic flow curves. In this context, the derivative of the curve is defined as the work hardening rate, i.e., the increase in stress necessary to achieve a specific deformation. The work hardening rate (θ), as per Equation 1, corresponds to the derivative of the stress versus equivalent strain curve (σ vs. ε) and tends to decrease with increasing temperature (T) and decreasing strain rate.

$$\theta = \frac{d\sigma}{d\varepsilon} \quad (1)$$

1.2.2 Dynamic Recovery (DRV)

The process of dynamic recovery occurs during plastic deformation, involving the restoration of the crystalline substructures formed by work hardening. These substructures are crystalline defects that develop due to the increased dislocation density during the initial deformation. Work hardening results in an accumulation of internal energy in the material. The energy for this process is provided by the internal energy stored in the material due to work hardening. Dislocations move and rearrange, seeking lower energy configurations. Normally, alloys with high stacking fault energy (SFE) tend to perform DRX (Jorge Jr and Balacin, 2005).

1.2.3 Dynamic Recrystallization (DRX)

Dynamic recrystallization is a softening process that occurs in metals with moderate or low SFE during deformation, resulting in a new, refined, and deformation-free microstructure. Controlling this process during processing is crucial to improving both the microstructural quality and the final properties of materials. In moderate or low SFE austenitic stainless steels, dislocations move further apart, reducing the effectiveness of climb and cross-slip mechanisms. This results in slower recovery, allowing the dislocation density to increase during deformation. In these cases, the rate of dislocation generation exceeds the rate of annihilation, leading the material to store a significant amount of energy in the substructures formed by work hardening. This energy stored during deformation acts as the driving force for dynamic recrystallization, increasing until a critical point is reached where the energy barrier is overcome, and nucleation mechanisms of new, deformation-free crystalline grains are initiated (Najafizadeh *et al*., 2006).

1.2.3.1 Determination of the Critical Stress for the Onset of Dynamic Recrystallization

From Equation 2, it is possible to determine the stress for the onset of dynamic recrystallization by identifying the inflection point of the third-degree curve, which plots the work hardening rate versus the equivalent stress (Poliak and Jonas, 1996).

$$\theta = A\sigma^3 + B\sigma^2 + C\sigma + D \quad (2)$$

where A, B, C, and D are constants.

By taking the derivative of the equation with respect to stress (σ), Equation 3 is obtained. The minimum of the derivative in Equation 3 represents the critical stress for the onset of dynamic re-crystallization (σ_c), as determined in Equation 4.

$$\frac{d\theta}{d\sigma} = 3A\sigma^2 + 2B\sigma + C \tag{3}$$

$$\frac{d^2\theta}{d\sigma^2} = 6A\sigma_c + 2B = 0 \Rightarrow \sigma_c = \frac{-B}{3A} \tag{4}$$

1.2.4 Stacking fault energy

Stacking Fault Energy (SFE) can be understood from its relation to its chemical composition and, consequently, to its crystal lattice. The number of dislocations in metals affects their ability to undergo plastic deformation, influencing the mechanical behavior during deformation and thus the final properties achieved. Dislocations are linear defects that move atoms during the plastic deformation of metals, leading to changes in the stacking order of atoms through the slip of adjacent crystallographic planes, resulting in stacking faults. These defects arise when a dislocation splits into two partial dislocations to reduce the energy required for its movement within the crystal lattice. The distance between these partial dislocations reaches an equilibrium determined by the stacking fault energy, which is estimated by considering the repulsive energy between the dislocations and the surface energy of the fault. According to dislocation theory, a stacking fault in a metal with a face-centered cubic (FCC) structure consists of an area with a different local crystalline arrangement, bounded by dissociated partial dislocations on a specific slip plane. In this case, the greater the separation distance (d) between two partial dislocations, the greater the width of the stacking fault, and consequently, the lower the SFE (Schram *et al.*, 1996), (Dieter, 1976).

2. MATERIALS AND METHODS

In this study, an austenitic stainless steel with a high nitrogen content was used, intended for the manufacture of orthopedic implants according to ISO 5832-9. The material was provided as rolled bars with a diameter of 20 mm, in the solution-annealed condition at 1030 °C for 60 minutes and water-cooled. The production involved an initial melting process in a Vacuum Induction Melting (V.I.M.) furnace followed by Electro Slag Remelting (E.S.R) under vacuum conditions. The chemical composition of the material by weight is detailed in the quality certificate provided by the manufacturer, as shown in Table 1.

TABLE 1. Chemical composition, by weight, of the main elements of the ISO 5832-9 steel produced by Villares S/A.

C	Si	Mn	Ni	Cr	Mo	S	P	Cu	N	Nb	Fe
0.017	0.16	3.62	10.6	21.06	2.44	0.0018	0.013	0.06	0.37	0.4	bal.

Source: Author (2024).

2.1 Hot Torsion Test

In the tests, the samples were heated by radiation to 1200 °C for 300 seconds and then cooled down to the testing temperature, ranging from 1000 °C to 1200 °C in 50 °C increments. At these temperatures, the specimens were held for 30 seconds and then deformed at a rate of 1.0 s^{-1}. All tests were conducted until the deformation reached 3.5 or until the sample failed. The tests were performed on the hot torsion machine at IFMA-Monte Castelo, Mechanical and Thermomechanical Testing Laboratory, Figure 5 (c).

2.2 Analytical method for obtaining stacking fault energy along the Stress vs. Strain curve

To find the SFE values for different points on the flow curve, the method proposed by Uesugi et al. (2012) was used, which relates the stacking fault energy with hot deformation factors, as shown in Equations 6 and 7.

$$\dot{\varepsilon} = A\left(\frac{\gamma_{sfe}}{\mu b}\right)^{3}\left(\frac{\mu b}{kT}\right)\left(\frac{\sigma_i}{\mu}\right)^{m} D_o \exp\left(-\frac{Q_o}{RT}\right) \quad (6)$$

$$\mu(T) = \mu_o\left[1 + \frac{(T-300)}{T_m}.\frac{T_m}{\mu_o}.\frac{d\mu}{dT}\right] \quad (7)$$

where $\dot{\varepsilon}$ is the strain rate, μ(T) is the shear modulus as a function of absolute temperature, μ_o = 8.1×10^{4} MN/m^2, b is the Burgers vector ($b_{Fe\text{-}\gamma}$ = 2.54×10^{-10} m), k is the Boltzmann constant, D_o is the pre-exponential factor for self-diffusion of γ-Fe, Q_o is the self-diffusion energy of austenite of 284 kJ/mol, R is the universal gas constant, T_m = 1810 K, and A and m are material-specific constants.

3. RESULTS AND DISCUSSION

Figure 6 shows the stress-strain curves obtained through continuous isothermal tensile testing. Initially, there is a progressive increase in stress, consistent with the phenomenon of work hardening (WH). This behavior is reproduced for all temperatures until there is a change in curvature due to softening processes (DRV and DRX), reaching a peak stress (σ_p). As deformation progresses past the peak, the stress tends to decrease and the curves approach a situation known as steady-state stress (σ_{ss}), where the dislocation creation rate equals the dislocation annihilation rate.

Furthermore, in Figure 6, it is observed that the higher the test temperature, the lower the stress peaks, since lower activation energies are required for deformation. Additionally, in these cases, as seen for temperatures from 1100°C to 1200°C, there is an abrupt change in curvature without a well-defined peak, which is consistent with the predominance of the dynamic recovery process (DRV). However, at lower temperatures, such as 1050°C and 1000°C, a well-pronounced peak is observed, indicating a greater effect of dynamic recrystallization (DRX) due to the higher accumulation of dislocations in the initial region of the curve.

FIGURE 6. Stress-strain curves from hot torsion tests of ISO 5832-9 steel.

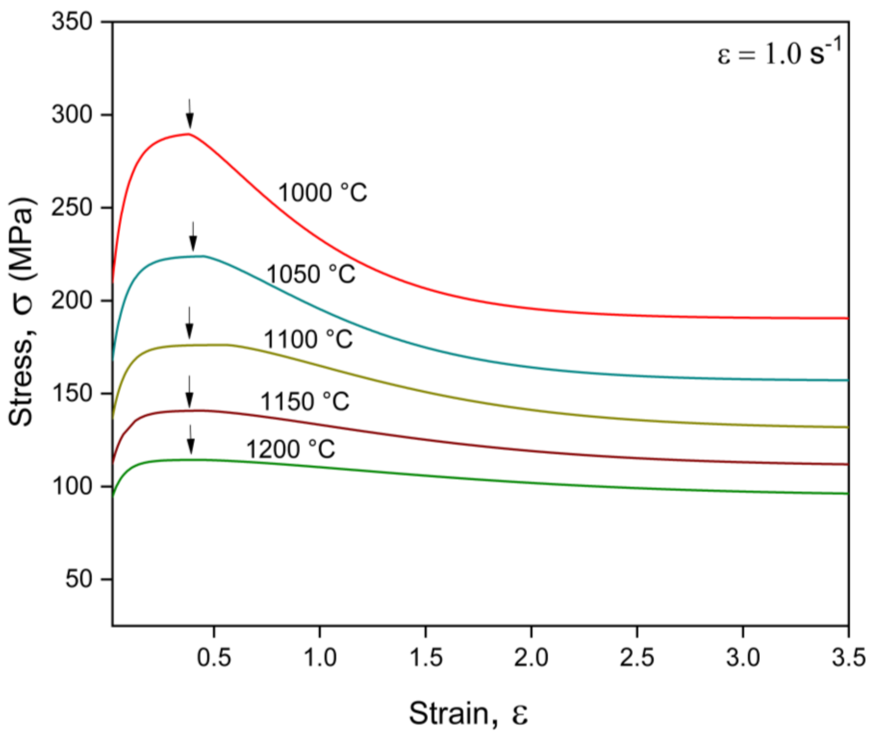

Source: Author (2024).

The graphical demonstration of the Poliak-Jonas (1996) method applied to the stress-strain curves in Figure 6 can be seen in Figure 7. In the graph, the work hardening rate (θ) is plotted against the stress, represented by the inflection point σ_c, which characterizes the onset of DRX. In this situation, it is not possible to accurately obtain the value of the critical stress; therefore, it is derived once more to be found through the minimum point in the -dθ/dσ relation. The saturation stress σ_{sat} is found by extending the curve at the inflection point until it intersects the abscissa at θ=0.

FIGURE 7. Graph of work hardening rate versus stress (a) and second derivative of work hardening rate as a function of stress (b)

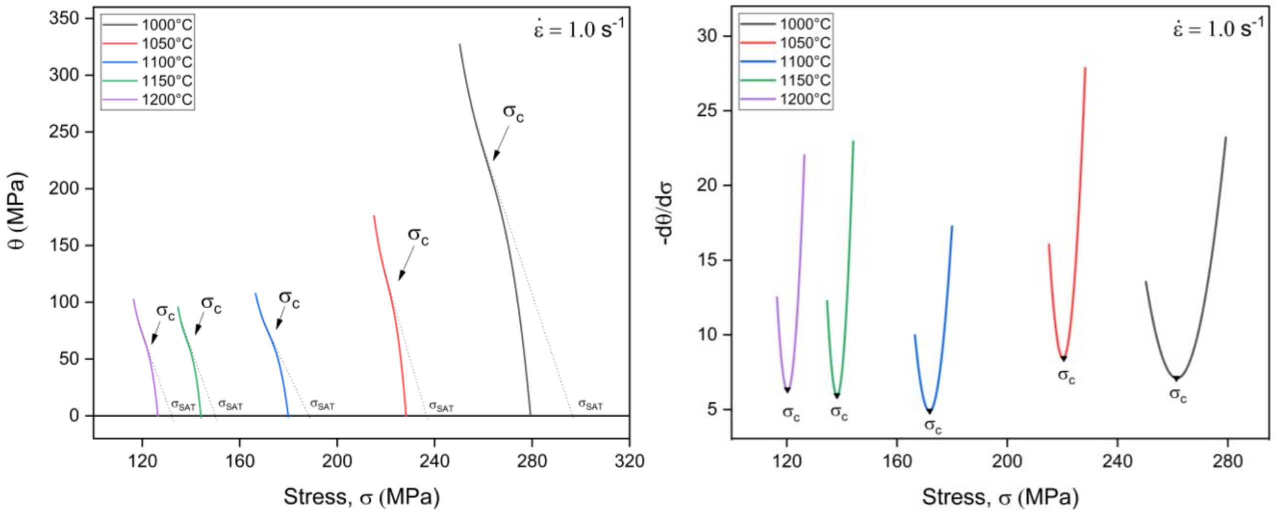

(a) (b)

Source: Author (2024).

Table 2 defines characteristic points of stress and strain along the plastic flow curves, obtained through the method proposed by Poliak-Jonas, using Equations 6 and 7. It is observed that the ratio σ_p/σ_c has an average value of 0.95, indicating that the onset stress of recrystallization is very close to the peak of the curve. This is due to the moderate value of the material's stacking fault energy γ_{sfe} = 68 mJ/m² (Aquino *et al.*, 2019), causing a delay in the nucleation of new grains and the consequent predominance of the recovery process. Furthermore, the average ratio σ_{sat}/σ_p = 1.03 shows that the maximum stress reached is very close to the saturation stress value, which would be the hypothetical stress if the material softened exclusively by dynamic recovery.

For the factor σ_{ss}/σ_p, an average ratio of 0.79 is observed, which aligns with the result of a material predominantly undergoing dynamic softening by recovery, given the small reduction in stress on the curve after the peak. Additionally, when examining the influence of temperature on this parameter, it is seen that the ratio σ_{ss}/σ_p approaches the value of 1, indicating that at higher temperatures, the material tends to recover dynamically with greater predominance.

TABLE 2. Parameters of the stress-strain curves of iso 5832-9 steel.

T °C	σ_p	ε_p	σ_c	ε_c	σ_{sat}	σ_{ss}	ε_{ss}	σ_p/σ_c	σ_{ss}/σ_p	$\sigma_{sa}t/\sigma_p$
1000 °C	279.29	0.38	261.63	0.18	292.40	178.66	3.88	0.94	0.64	1.05
1050 °C	228.29	0.39	220.20	0.22	234.09	167.32	2.92	0.96	0.73	1.03
1100 °C	179.97	0.57	171.74	0.30	186.57	146.14	2.62	0.95	0.81	1.04
1150 °C	144.14	0.45	138.32	0.24	147.57	122.95	2.21	0.96	0.85	1.02
1200 °C	126.43	0.39	120.32	0.19	130.83	118.23	3.06	0.95	0.94	1.03
AVERAGE	191.62	0.43	182.44	0.22	198.29	146.66	2.94	0.95	0.77	1.03

SOURCE: Author (2024).

Figure 8 shows the variation of stacking fault energy along the stress-strain curve, according to the methodology proposed by UESUGI et al (2012). It is observed that the energy starts at high values, around 65 to 75 mJ/m², decreases to a minimum value, from 10 to 20 mJ/m², which corresponds to the peak stress, and then increases again to intermediate values without significant variations after reaching the steady-state stress.

FIGURE 8. Stacking fault energy along the stress-strain curves

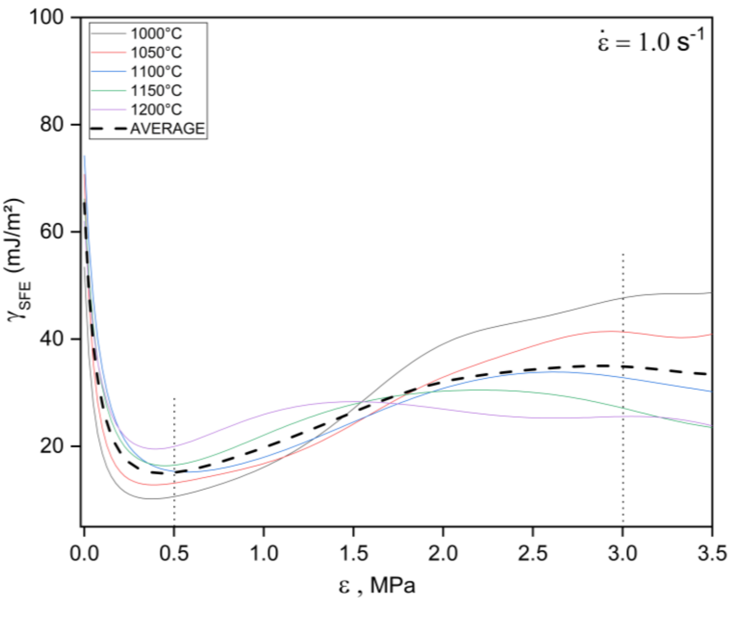

Source: Author (2024).

Figure 9 shows the variation of stacking fault energy with temperature for two different strains: ε = 0.5 and ε = 3.0; peak strain and steady-state strain, respectively. It is observed that for strain ε = 0.5, the stacking fault energy is higher as the test temperature increases, which may favor DRV at this point. However, in the steady-state, the situation reverses, and at higher test temperatures, the stacking fault energy is reduced, suggesting a relative predominance of DRX for high deformation.

FIGURE 9. Variation of stacking fault energy with temperature for strains (a) 0.5 and (b) 3.0

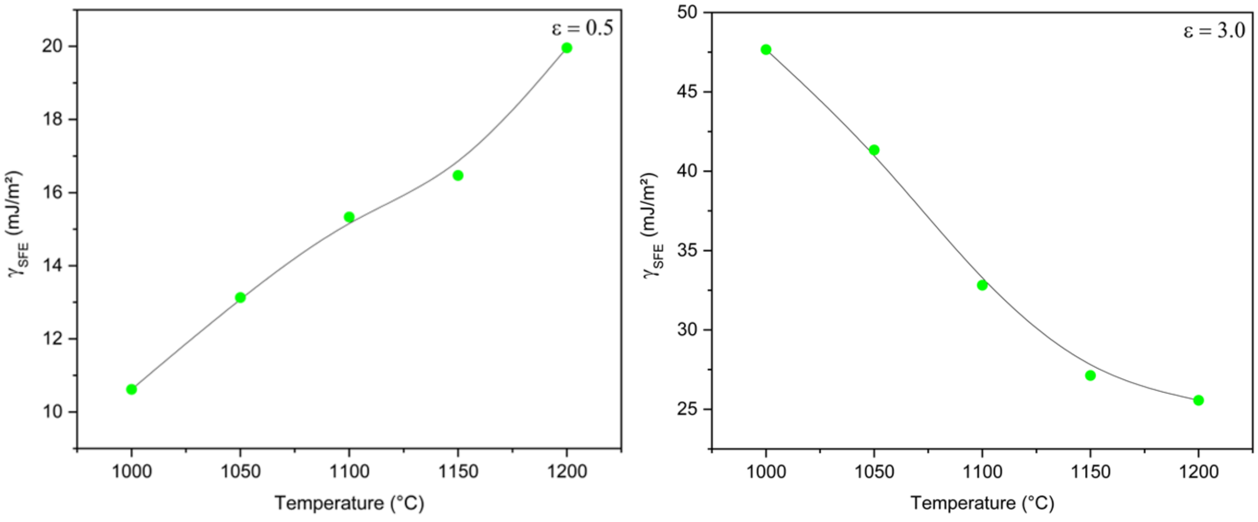

(a) (b)

SOURCE: Author (2024).

4. CONCLUSIONS

I. Results show that temperature greatly influences the stress levels of the plastic flow curves, even defining which softening mechanism (DRV or DRX) predominates in relation to their shape; for higher temperatures, DRV is more intense.

II. The characteristic stress and strain points of the stress-strain curves obtained through the method proposed by Poliak and Jonas indicate that the material tends to predominantly undergo dynamic recovery, which is consistent with its moderate stacking fault energy value.

III. The stacking fault energy varies along the stress-strain curve and is influenced by temperature: increasing at the peak stress and decreasing in the steady-state.

STATEMENT OF RESPONSIBILITY

The authors are solely responsible for this work.

REFERENCES

BALANCIN, O. Simulação Física Do Processamento A Quente De Materiais Metálicos. In: 67 ABM INTERNATIONAL CONGRESS, Rio de Janeiro, RJ, 2012. Abm Proceedings. p. 599-610. ISSN: 2594-5327, DOI 10.5151/2594-5327-20944

DE AQUINO, FELIPE ANDERSON S.; SILVA, EDEN S.; RODRIGUES, SAMUEL F.; ARANAS, CLODUALDO; SICILIANO, FULVIO; COUTINHO, SAMIR S.; REIS, GEDEON S. Thermomechanical Behavior of Biocompatible Austenitic Stainless Steels during Simulated Torsion Tests. JOURNAL OF MATERIALS ENGINEERING AND PERFORMANCE, v. 28, p. 5890-5901, 2019.

DIETER, E. G. Mechanical Metallurgy, 2nd ed., McGraw-Hill, 1976.

DE SOUSA SULZBACH, Gláucia Adriane et al. Constitutive analysis of stress–strain curves in dynamic softening of high Nb-and N-containing austenitic stainless-steel biomaterial. Journal of Materials Research and Technology, v. 19, p. 4939-4956, 2022.

FIELDS, D. S. e BACKOFEN, W. A. Determination of Strain Hardening Characteristics by Torsion Testing. Proc. Amer. Soc. Test. Mater. v. 57. p. 1263, 1957.

GERONIMO, F. H. C. Caracterização microestrutural e modelagem do amaciamento dinâmico a quente do aço inoxidável austenítico ASTM F 138, utilizado em implantes ortopédicos. 2014, 157 p. Tese (Doutorado em Ciência e Engenharia de Materiais) – PPGCEM/UFSCAR.

JORGE Jr., A. M. Análise do Comportamento Plástico Mecânico dos Aços Inoxidáveis em Altas Temperaturas e Altas Taxas de Deformação. (Tese de Doutorado). Programa de Pós Graduação em Ciência e Engenharia de Materiais, Universidade Federal de São Carlos, 1997.

JORGE Jr., A. M., BALANCIN, O. Prediction of Steel Flow Stresses Under Hot Working Conditions. Materiais Research, Vol. 8, No. 3, p. 309-315, 2005.

NAJAFIZADEH, A., JONAS, J. J. Predicting the Critical Stress for Initiation of Dynamic Recrystallization. ISIJ International, v. 46, No. 11, p. 1679-1684, 2006.

POLIAK, E. I. e JONAS, J. J. A One Parameter Approach to Determining the Critical Conditions for the Initiation of Dynamic Recrystallization. Acta Metallurgica, v. 44, No. 1, p. 127-136, 1996.

SCHRAM, R. E., REED, R. P. Stacking fault energy of seven commercial austenitic stainless steels. Metallurgical Transactions 6A, p. 1345, 1966.

SILVA, E. S. Caracterização e modelagem do comportamento plástico a quente do aço inoxidável austenítico ISO 5832-9, utilizado em implantes ortopédicos. 2011, 221 p. Tese (Doutorado em Ciência e Engenharia de Materiais) – PPGCEM/UFSCAR.

SILVA, E. S. et al. Hot deformation behavior of a Ni-bearing austenitic stainless steel biomaterial. In: 67 ABM INTERNATIONAL CONGRESS, Rio de Janeiro, RJ, 2012. Abm Proceedings. p. 391-402. ISSN: 2594-5327, DOI 10.5151/2594-5327-20909.

Uesugi et al, Advanced Technologies, Inc, Japan, 2012. 412-0047. http://www.ati-mt.co.jp/en/pg237.html. Accessed 19 Nov 2018.

ACKNOWLEDGMENTS

The authors thank the Federal Institute of Maranhão (IFMA), and Postgraduate Program in Science and Technology of Materials and the Brazilian funding agencies, CAPES (88887.959941/2024-00), FINEP (33.749.086/0001-09) e à FAPEMA (07168/22).